Langmuir

ARTICLE

pubs.acs.org/Langmuir

Mutable Lewis and Brønsted Acidity of Aluminated SBA-15 as Revealed by NMR of Adsorbed Pyridine-^{15}N

Andrey A. Gurinov,[†,‡] Yulia A. Rozhkova,[‡] Arnošt Zukal,[§] Jiří Čejka,[*,§] and Ilya G. Shenderovich[*,†,‡]

[†]Institut für Chemie und Biochemie, Freie Universität Berlin, Takustraße 3, 14195 Berlin, Germany

[‡]Department of Physics, St. Petersburg State University, Ulianovskaya 1, 198504 St. Petersburg, Russian Federation

[§]J. Heyrovský Institute of Physical Chemistry, Academy of Sciences of the Czech Republic, v.v.i. Dolejškova 3, CZ-182 23 Prague 8, Czech Republic

ABSTRACT: ^{1}H and variable-temperature ^{15}N NMR techniques have been used to study the effect of the gradual alumination of SBA-15 on the structure and adsorption properties of this mesoporous material. The interpretation of experimental spectra suggests that aluminum chlorhydrol most effectively reacts with silica surfaces in the confinement of the cavities of rough mesopore walls, instead of forming a homogeneous aluminum film. This first leads to a gradual filling of the cavities and finally results in aluminum islands on the inner surfaces of mesopores. In the sample with a Si/Al atomic ratio of 4.1, up to half of the inner surface area of the mesopores is covered with aluminum. The alumination produces Brønsted acid sites attributed to silanol groups interacting with aluminum but does not affect the proton-donating ability of isolated silanol groups. At high Si/Al ratios, the surface contains only one type of Lewis site attributed to tetracoordinated aluminum. At lower Si/Al ratios, Lewis acid sites with a lower electron-accepting ability appear, as attributed to pentacoordinated aluminum. The numerical values of the surface densities of all chemically active sites have been estimated after annealing at 420 and 700 K. We were surprised to observe that gaseous nitrogen can occupy Lewis acid sites and hinder the interaction of the aluminum with any other electron donor. As a result, aluminated surfaces saturated with nitrogen do not exhibit any Brønsted or Lewis acidity. At room temperature, it takes days before pyridine replaces nitrogen at the Lewis acid sites.

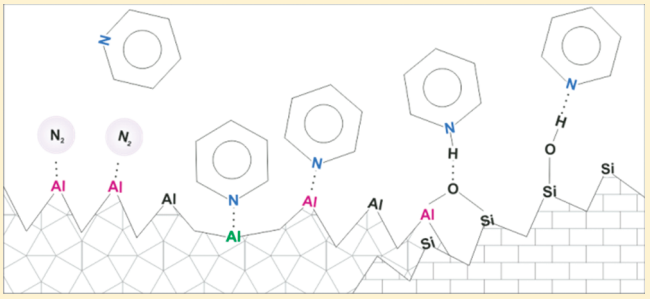

1. INTRODUCTION

The main advantage of ordered mesoporous silicas is that they offer extremely high surface areas whose catalytic function can be selectively varied. One can either deposit or bind covalently active species to the inner surfaces or incorporate active sites into the silica walls.[1−6] In the two former cases, the effect of the surface on the chemical reactivity and the accessibility of the active species can be neglected.[7,8] By contrast, the incorporation of active sites into the silica walls can affect the chemical reactivity of both the introduced sites and the surrounding surface. Probably the most elaborated upon example of such a modification is alumination. When a silicon atom is isomorphously substituted for an aluminum atom, a negative charge should be introduced into the framework.[5] However, in reality the effect of this substitution depends on many parameters.[9] There is a considerable discrepancy between both the experimental results obtained and their interpretation.[10−16] It is not clear how many different types of Lewis acid sites can coexist on aluminated surfaces.[11−17] Most of authors support the view that alumination creates strong Brønsted acid groups because of the interaction of the oxygen atoms of surface silanol groups with neighboring aluminum atoms.[10,11,15,16] It is remarkable that the formation of such acidic groups requires the hydrogen bonding of the silanol group to an external proton acceptor.[10] The proton-donating ability of these groups is then sufficient to protonate bases such as trimethylphosphine.[14,15] It should be noted, however, that strong bases also become protonated on pure siliceous surface of MCM-41 because of the mutual interactions of silanol groups.[18]

If calcined SBA-15 material containing octahedrally coordinated extraframework aluminum is treated with a solution of NH_4OH, then aluminum is inserted into tetrahedral framework positions.[19,20] Recently, some of us have observed a notable effect of alumination on the surface roughness of mesoporous silica.[21] The successive grafting of aluminum on SBA-15 has led to a gradual filling of the cavities of rough mesopore walls. As a consequence, a smoothing of the mesopore surface has taken place. Generally, the postsynthesis modification can vary the density and the accessibility of surface hydroxyl groups.[22]

We are aware of the application of ^{31}P NMR of phosphines to the characterization of acidic sites of aluminated silicas.[13,14] However, in this study we are using for the same purposes ^{15}N NMR of pyridine because its chemical shift can be used to

Received: May 10, 2011
Revised: July 8, 2011
Published: August 22, 2011

Table 1. Structural Features of Mesoporous Silicas Studied in This Work Adjusted from Reference 21

silica	S_{BET}, m^2/g[a]	$m_{Al_2O_3}$, wt %[b]	Si/Al[c]	^{27}Al NMR[d]
SBA-15/0	805.9		∞	
SBA-15/8	618.3	6.9	11.5	T, O
SBA-15/48	456.1	16.2	4.4	T, O, P
SBA-15/64	445.4	17.1	4.1	T, O, P

[a] BET specific surface area. [b] Amount of Al_2O_3 in aluminated SBA-15. [c] Atomic ratio. [d] T, O, and P stand for tetrahedral, octahedral, and pentahedral aluminum atoms, respectively.

estimate numerically the geometries of hydrogen-bonded complexes between pyridine and Brønsted acid groups.[23] Variable-temperature ^{15}N NMR experiments can provide information about the dynamics of adsorbed molecules,[18] their orientation at the surface,[24,25] and what is specifically important for this study pertaining to information about the surface roughness of different mesoporous silicas.[24] The effect of the formation of Lewis acid−base complexes on the ^{15}N chemical shift of pyridine is known as well.[26−28]

The goal of this work is to study the effect of the gradual alumination of SBA-15 on the properties of host−guest interactions. We expect that an inspection of these properties will make it possible to characterize the local morphology of the inner surfaces of the resulting materials. In particular, it is not clear whether ^{15}N NMR of adsorbed pyridine can be used to discriminate between surface-smooth and surface-corrugated SBA-15 materials, as has been done for MCM-41 silicas.[24]

Three types of measurements have been proposed and carried out to characterize purely siliceous and aluminated SBA-15 silicas: (1) ^{15}N NMR at 130 K under magic angle spinning (MAS) conditions at a submonolayer and high loading of pyridine-^{15}N to identify different adsorption-active sites; (2) ^{15}N NMR at 300 K under static conditions at a submonolayer loading of pyridine-^{15}N to estimate the surface roughness from the residual ^{15}N chemical shift anisotropy; and (3) ^{1}H MAS NMR at 300 K in the presence and absence of pyridine-d_5 to analyze the effect of grafting on the accessibility of silanol groups.

2. EXPERIMENTAL SECTION

2.1. Materials and Samples. Aluminum-grafted materials were prepared from purely siliceous SBA-15. Specific details of the synthesis and the structural characteristics of these materials were reported in ref 21. Structural features of mesoporous silica materials studied in this work are collected in Table 1. These samples are labeled as SBA-15/*c*, where *c* denotes the concentration of aluminum chlorhydrol in the grafting solution. In some NMR experiments, we used commercially available MCM-41 and Al-MCM-41 materials purchased from Sigma-Aldrich, labeled here as MCM-41 and Al-MCM-41 samples, and a sample of purely siliceous SBA-15 loaded with pyridine-^{15}N. The last sample was sealed in a glass insert (Wilmad, Buena, NY) for Chemagnetics 6 mm rotors and was the same sample as sample d in ref 24. This sample is labeled here as SBA-15/d. Pyridine-^{15}N (98% enriched) was synthesized in our laboratory from ammonium chloride (^{15}N, 99%, Cambridge Isotope Laboratories, Inc.), and pyridine-d_5 (99% enriched) was purchased from Euriso-Top.

Samples for NMR measurements SBA-15/*c*-a and SBA-15/*c*-b were prepared as follows: to remove physisorbed and hydrogen-bonded water without causing the dehydroxylation of silanol groups, silica material was dried in vacuo (10^{-3} Pa) at 420 K for >18 h inside a 6 mm NMR rotor, which afterward was placed in a glovebag where the calculated amount of water-free pyridine was added under an argon atmosphere. Because there was an open Dewar vessel with liquid nitrogen inside the glovebag, the atmosphere contained an uncontrollable amount of gaseous nitrogen as well. The NMR rotor was kept tightly closed for 12 h to ensure a homogeneous distribution of the pyridine molecules in the pores. Samples for NMR measurements SBA-15/*c*-c and SBA-15/*c*-d were prepared similarly to sample SBA-15/d as described in ref 24. Physisorbed and hydrogen-bonded water was removed from the samples in vacuo (10^{-3} Pa) at either 700 K (SBA-15/*c*-c) or 420 K (SBA-15/*c*-d) for >18 h inside a glass insert (Wilmad, Buena, NY) for Chemagnetics 6 mm rotors. A calculated amount of pyridine-^{15}N was loaded by vacuum transfer, and the glass insert was flame sealed to prevent any contact with the environment. The most important features of the NMR samples are given in Table 2.

A sample for FTIR measurement SBA-15/48-a was prepared as follows. Prior to the adsorption of pyridine molecules, a self-supporting wafer was activated in situ by evacuation at 720 K overnight at 2.5×10^{-2} Pa. The adsorption of pyridine proceeded at 420 K for 20 min at a

Table 2. Samples of Mesoporous Silicas Loaded with Pyridine-^{15}N Studied in This Work

		resonances in ^{15}N NMR, ppm		
sample	pyridine per nm^2[a]	at 300 K	at 130 K	species per nm^2 at 130 K[b]
SBA-15/0-a	0.3	258	258	0.3
SBA-15/0-b	4.0		276	1.9
			258	2.1
SBA-15/8-a	0.3	251	258	0.3
SBA-15/8-b	4.0	263	276	2.0
			258	1.3
			251	0.7
SBA-15/8-c	5.6		276	1.9
			258	2.7
			200	0.2
			167	0.8
SBA-15/64-a	0.3	251	258	0.3
SBA-15/64-b	4.0	263	276	2.2
			258	1.0
			251	0.8
SBA-15/64-b[c]	4.0	233	233	
		200	200	
			167	
SBA-15/64-c	9.2		276	4.7
			258	1.6
			233	1.1
			200	1.3
			167	0.5
SBA-15/64-d	3.3	264	276	0.3
		200	258	1.2
		167	233	0.3
			200	0.3
			167	1.2
SBA-15/d	1.7	254	252	1.7

[a] Total number of loaded pyridine molecules per nm^2 of BET specific surface area. [b] Calculated from the integral intensities of ^{15}N NMR spectra at 130 K. [c] Spectral changes after 60 days.

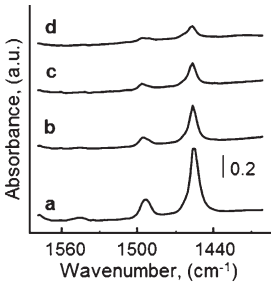

Figure 1. Characteristic IR bands of pyridine on Lewis (1455 cm^{-1}) and Brønsted (1545 cm^{-1}) acid sites after desorption at (a) 420, (b) 520, (c) 620, and (d) 720 K. The numbers of pyridine molecules adsorbed on Lewis and Brønsted acid sites per nm^2 are (a) 0.40 and 0.03, (b) 0.19 and 0.01, (c) 0.14 and <0.01, and (d) 0.05 and <0.01, respectively. The band at 1491 cm^{-1} corresponds to another vibration of pyridine bound to these acid sites.

partial pressure of 650 Pa followed by 20 min of evacuation at the same temperature.

2.2. FTIR Measurements. The concentration and type of acid sites were determined by the adsorption of pyridine as a probe molecule, followed by FTIR spectroscopy on a Nicolet 6700 FTIR spectrometer using the self-supported wafer technique. The spectra were recorded with a resolution of 4 cm^{-1} by collecting 128 scans for a single spectrum.

2.3. NMR Measurements. ^{1}H MAS NMR measurements were carried out on a Varian Infinity Plus 600 spectrometer operating at 14 T, equipped with a variable-temperature Chemagnetics-Varian 4 mm pencil CPMAS probe, employing a 90° pulse length of 3.5 μs, a recycle delay of 5 s, and MAS at 10 kHz. ^{1}H chemical shifts are referenced to trimethylsilyl-2,2,3,3-tetradeuteropropionic acid (TSP, sodium salt).

^{15}N NMR measurements were performed on a Bruker MSL-300 instrument operating at 7 T, equipped with a variable-temperature Chemagnetics-Varian 6 mm pencil CPMAS probe. The {^{1}H}-^{15}N spectra under MAS and static and cross-polarization (CP) conditions were recorded using a typical 90° pulse length of 4.0 μs, a recycle delay of 20 s, and a contact time of 5 ms. Under MAS conditions, the samples were spun at 6 kHz. ^{15}N chemical shifts are referenced to the solid $^{15}NH_4Cl$ scale.

3. RESULTS

In this section, the results of FTIR and NMR experiments are reported, and the interpretation of the obtained results follows in the Discussion section. Variable-temperature ^{15}N NMR under MAS conditions was used to inspect the state of pyridine-^{15}N accommodated in mesoporous silicas under different conditions. ^{15}N NMR at 300 K under static conditions was used to estimate the residual ^{15}N chemical shift anisotropy of adsorbed pyridine, and ^{1}H NMR was applied to characterize the accessibility of silanol groups. It should be noted that the ^{15}N NMR resonance of bulk frozen pyridine is at 276 ppm[24] and the ^{1}H NMR resonance of isolated silanol groups is at 1.8 ppm.[29]

3.1. FTIR. Figure 1 shows characteristic IR bands of pyridine interacting with Brønsted (1545 cm^{-1}) and Lewis (1455 cm^{-1}) acid sites. The number of pyridine molecules adsorbed on these sites depends on the temperature and can be estimated from the integral intensities of the individual bands and the molar absorption coefficients ε(Brønsted) = 1.7 ± 0.1 cm μmol^{-1} and ε(Lewis) = 2.2 ± 0.1 cm μmol^{-1}.[30] The band at 1491 cm^{-1} corresponds to another vibration of pyridine bound to these acid sites, and its intensity does not provide any new information.

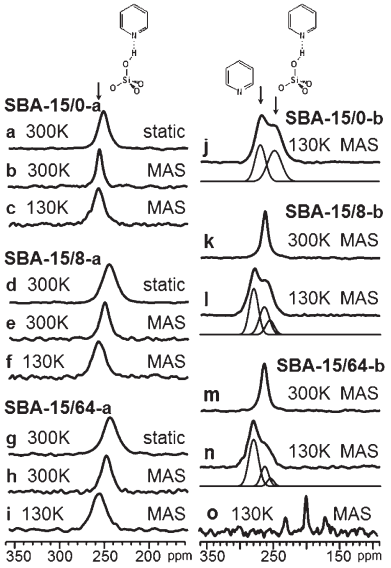

Figure 2. ^{15}N NMR spectra of SBA-15 loaded with a submonolayer of pyridine-^{15}N in a glovebag under an argon/nitrogen atmosphere: (a) SBA-15/0-a at 300 K, static conditions; (b) SBA-15/0-a at 300 K, MAS; (c) SBA-15/0-a at 130 K, MAS; (d) SBA-15/8-a at 300 K, static conditions; (e) SBA-15/8-a at 300 K, MAS; (f) SBA-15/8-a at 130 K, MAS; (g) SBA-15/64-a at 300 K, static conditions; (h) SBA-15/64-a at 300 K, MAS; and (i) SBA-15/64-a at 130 K, MAS. ^{15}N NMR spectra, experimental (upper) and deconvolution (lower), of SBA-15 loaded with excess pyridine-^{15}N: (j) SBA-15/0-b at 130 K, MAS; (k) SBA-15/8-b at 300 K, MAS; (l) SBA-15/8-b at 130 K, MAS; (m) SBA-15/64-b at 300 K, MAS; (n) SBA-15/64-b at 130 K, MAS; (o) SBA-15/64-b at 130 K, MAS, after 60 days.

3.2. ^{15}N NMR. ^{15}N NMR spectra of SBA-15/0, SBA-15/8, and SBA-15/64 materials loaded with submonolayers of pyridine-^{15}N in a glovebag under an argon/nitrogen atmosphere are depicted in Figure 2a–i. For purely siliceous SBA-15/0, the position of the resonance, 258 ppm, does not depend on the temperature (Figure 2b,c and Table 2). In contrast, for aluminated SBA-15/8 and SBA-15/64 the position of the resonance does depend on the temperature (Figure 2e,f and Figure 2h,i, respectively). These values are 251 ppm at 300 K and 258 ppm at 130 K, respectively. Spectral lines in static spectra are broader than MAS spectra but isotropic for all samples (Figure 2a,d,g and Figure 2b,e,h).

^{15}N NMR spectra of the same samples loaded with excess pyridine-^{15}N in a glovebag under an argon/nitrogen atmosphere are presented in Figure 2j–o. For all samples, the amount of pyridine is about 4 molecules per nm^2 on the surface. For purely siliceous SBA-15/0, the spectrum at 130 K can be deconvoluted in two signals centered at 276 and 258 ppm (Figure 2j). For aluminated SBA-15/8 and SBA-15/64, a third signal is needed in order to reproduce the experimental line shape. This signal is tentatively placed at 251 ppm (Figure 2l,n). Although the total amount of pyridine resonating at 258 ppm decreases upon an increase in the Al content, the amount of pyridine resonating at 251 ppm increases (Table 2). At 300 K, the only signal is at 263 ppm (Figure 2k,m). Sample SBA-15/64-b was accidentally left in a tightly closed NMR MAS rotor for 60 days. The spectrum of this sample at 130 K reveals dramatic changes (Figure 2o). The total integral intensity of the ^{15}N resonances decreases strongly, indicating the slow evaporation of pyridine from the NMR rotor.

dx.doi.org/10.1021/la2017566 |*Langmuir* 2011, 27, 12115–12123

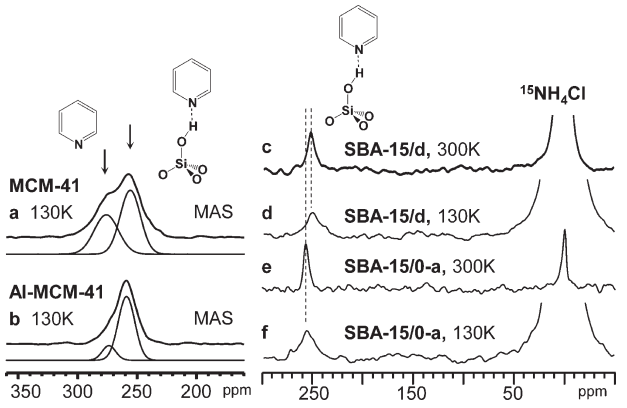

Figure 3. ^{15}N NMR spectra, experimental (upper) and deconvolution (lower), of MCM-41 and Al-MCM-41 loaded with excess pyridine-^{15}N: (a) MCM-41 at 130 K, MAS and (b) Al-MCM-41 at 130 K, MAS. ^{15}N NMR spectra of SBA-15 loaded with a submonolayer of pyridine-^{15}N in the presence of $^{15}NH_4Cl$ as an internal reference for the chemical shift: (c) SBA-15/d at 300 K, MAS; (d) SBA-15/d at 130 K, MAS; (e) SBA-15/0-a at 300 K, MAS; and (f) SBA-15/0-a at 130 K, MAS.

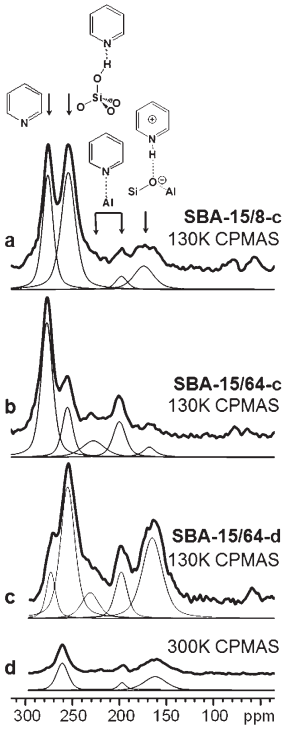

Figure 4. ^{15}N NMR spectra, experimental (upper) and deconvolution (lower), of SBA-15 loaded with excess pyridine-^{15}N under vacuum: (a) SBA-15/8-c at 130 K, CPMAS; (b) SBA-15/64-c at 130 K, CPMAS; (c) SBA-15/64-d at 130 K, CPMAS; and (d) SBA-15/64-d at 300 K, CPMAS.

However, there remain three well-resolved signals at 233, 200, and 167 ppm.

For comparison, the ^{15}N NMR spectra of commercially available MCM-41 and Al-MCM-41 silicas loaded with excess of pyridine-^{15}N have been obtained at 130 K (Figure 3a,b). The shapes of the obtained experimental spectra can be reproduced using only two partially overlapping resonances centered at 276 and 258 ppm.

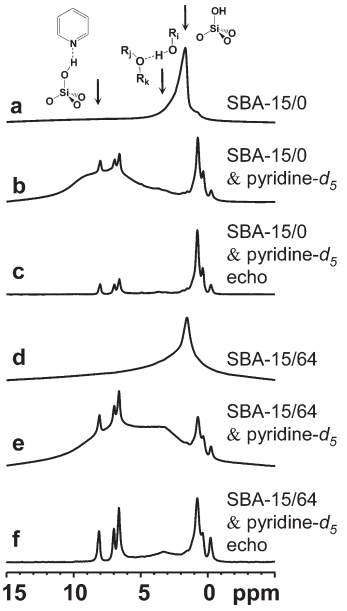

Figure 5. ^{1}H MAS NMR spectra at 300 K of (a) SBA-15/0 and (d) SBA-15/64 and the same silicas loaded with excess ring-deuterated pyridine-d_5, (b, c and e, f, respectively). (c, f) The spectra were obtained under the spin−echo conditions with τ = 824 μs. The spectra do not exhibit any signal outside the region shown up to 30 ppm. The signals below 1 ppm in the pyridine-d_5-loaded samples are attributed to trace amounts of vacuum grease.

Because the position of the resonance detected for sample SBA-15/0-a differs from the position of resonances obtained for similar systems in the past,[24] we have compared the ^{15}N spectra of SBA-15/0-a and SBA-15/d in the presence of $^{15}NH_4Cl$ as an internal reference (Figure 3c−f). Indeed, at both 300 and 130 K pyridine resonates at 258 ppm when it is adsorbed onto SBA-15/0 and at 252 ppm when it is adsorbed onto SBA-15/d.

^{15}N NMR spectra of SBA-15/8 and SBA-15/64 loaded with excess pyridine-^{15}N by vacuum transfer are depicted in Figure 4a−d. Under CPMAS conditions at 130 K, all spectra contain signals at 276, 258, 200, and 167 ppm. In the case of SBA-15/64, there is one more signal located at 233 ppm (Figure 4b,c). At 300 K, at the expense of the low-temperature resonances at 276 and 258 ppm, there appears a signal at 264 ppm (Figure 4d).

3.3. ^{1}H NMR. Figure 5 shows the ^{1}H MAS NMR spectra obtained at 300 K for SBA-15/0 and SBA-15/64 samples evacuated at 420 K and the same materials loaded with excess pyridine-d_5. In the absence of the guest, a resonance at 1.7 ppm dominates for both samples (Figure 5a,d). A broad shoulder centered near 3 ppm is observed in both spectra but is more pronounced for SBA-15/64. In the presence of pyridine, the resonance at 1.7 ppm disappears completely and a broad line covering the region from 10 to 5 ppm is observed (Figure 5b,e). The broad signal at 3 ppm remains, but the effect of the guest on the amplitude of this signal has not been defined. The amplitude of this signal in SBA-15/64 is higher as compared with that in SBA-15/0, which is especially pronounced in spectra obtained under spin−echo conditions using a long echo delay (Figure 5c,f). Sharp signals presented in the spectra of the pyridine-d_5-loaded samples between 9 and 6 ppm are attributed to residual aromatic protons of the pyridine molecule, and those below 1 ppm are attributed to trace amounts of vacuum grease.

4. DISCUSSION

The main results of the experiments described above can be summarized as follows. The concentrations of Brønsted and Lewis acid sites calculated from the integral intensities of individual IR bands of adsorbed pyridine depend dramatically on the temperature, at which pyridine had been desorbed before the measurements. The numbers of pyridine molecules adsorbed on the Lewis and Brønsted acid sites per nm^2 after desorption at 420, 520, 620, and 720 K are 0.40 and 0.03, 0.19 and 0.01, 0.14 and <0.01, and 0.05 and <0.01, respectively. Thus, the measurements at 420 K provide only the lower limits of the concentrations of the Brønsted and Lewis acid sites.

The ^{15}N NMR spectral features depend mostly on the way in which pyridine had been loaded onto sample rather than on the material itself. For this reason, we consider separately the results obtained for samples loaded with pyridine under an argon/nitrogen atmosphere and by vacuum transfer.

We start the interpretation of the obtained data with a few remarks on the effect of adsorption onto mesoporous silicas on the spectral features of ^{15}N NMR of pyridine. On purely siliceous MCM-41 and SBA-15, pyridine forms hydrogen-bonded complexes with surface silanol groups. The isotropic ^{15}N chemical shift of the hydrogen-bonded pyridine depends on the N···H distance.[23] This interaction results in a high-field shift of 25 ppm relative to bulk pyridine.[24] An interaction of pyridine with strongly acidic groups grafted on silica surfaces causes a high-field shift of 100−110 ppm,[8] and a complete protonation should result in a high-field shift of about 125 ppm relative to bulk pyridine.[31]

Below a submonolayer loading, pyridine molecules jump rapidly between the surface silanol groups at room temperature but do not leave the surface. As a result, ^{15}N experiments on static samples of highly ordered MCM-41 silica show residual ^{15}N chemical shift anisotropy indicating that the reorientational diffusion of the adsorbed pyridine molecules is anisotropic. A quantitative analysis of this residual anisotropy revealed that in this regime the rotation of pyridine around the molecular C_2 axis is suppressed even at room temperature.[24]

In the presence of excess water, pyridine can form hydrogen-bonded complexes with different structures at silica surfaces, as manifested by a broad set of signals in low-temperature ^{15}N NMR spectra.[24] In the presence of a small amount of water, 2:1 pyridine/water complexes are formed.[18] This interaction should result in a high-field shift of the ^{15}N resonance of 14 ppm when related to the resonance of bulk pyridine.[32]

The density of the silanol groups depends on the type of mesoporous silica. The reported values are 2.9 and 3.7 groups per nm^2 for MCM-41 and SBA-15, respectively.[24]

4.1. Interaction of the SBA-15 Surface with Pyridine Loaded as a Drop under an Argon/Nitrogen Atmosphere. Purely siliceous SBA-15/0 exhibits, after the adsorption of pyridine, two different resonances at 130 K (Figure 2j). The one at 276 ppm belongs to frozen bulk pyridine, and the other at 258 ppm should be attributed to pyridine hydrogen bonded to silanol groups. We are surprised that the proton-donating ability of the silanol groups of SBA-15/0 is lower than that of previously studied MCM-41 and SBA-15 silicas.[24] However, the difference can be experimentally proven (Figure 3c−f). Thus, the proton-donating ability of the silanol groups of SBA-15/0 is comparable to the proton-donating ability of an acid, exhibiting an apparent pK_a value of about 5.0. The N····H distance in the pyridine−silanol pairs is about 1.7 Å.[23] The maximal number of pyridine molecules hydrogen bonded to the surface of SBA-15/0 is 2.1 per nm^2, as can be estimated from the integral intensities of the signals in Figure 2j. We associate this value with the density of the surface silanol groups. This value differs from that reported in the past, 3.7 per nm^2.[24] The observed differences in the proton-donating abilities and the densities of the silanol groups are probably related to either the synthesis or more probably the conditions of postsynthesis treatment and can be a consequence of slightly different structural features of the materials, as explained below.

The alumination of parent SBA-15 does not dramatically affect the density of the surface silanol groups that are accessible to pyridine (Table 2). Although the ratios of the surface areas available for nitrogen adsorption in SBA-15/0, SBA-15/8, and SBA-15/64 are 1:0.77:0.55 and the atomic Si/Al ratios are ∞:11.5:4.1, the ratio of the total densities of the silanol groups accessible to pyridine is 1:0.95:0.86. This trend can be understood if we assume that (i) some parts of SBA-15/0 surface, which are accessible to nitrogen, remain inaccessible to pyridine molecules and (ii) aluminum species most effectively react with the silica surface in the strongly confined geometry of the cavities of rough mesopore walls, where they can form conjugated covalent bonds to the surface[8] instead of forming a homogeneous film at the surface. The second assumption implies that the structure of SBA-15/64 should be free from hardly accessible cavities and that the surface areas accessible to nitrogen and pyridine are equal. Therefore, the lower limit of the surface area of SBA-15/0 accessible to pyridine is 450 m^2/g. In such a case, the upper limit of the density of the surface silanol groups in SBA-15/0 can be about 2.1 $nm^{-2}(806\ m^2/g)/450\ m^2/g = 3.8\ nm^{-2}$ (Table 2). The latter value is close to the values reported in the past for other mesoporous silicas.[24] The total density of the surface silanol groups in SBA-15/64 estimated from the pyridine adsorption is 1.8 per nm^2, in contrast to the upper-limit value of 3.8 per nm^2. However, the former value has been calculated without any correction for the presence of alumina areas on the surfaces. Within the framework of our assumptions, the alumination results in a gradual filling of the cavities of rough mesopore walls that finally leads to aluminum islands on the inner surfaces of mesopores.[21] The rest of the surface can be treated, at least to a first approximation, as purely siliceous with a surface silanol group density of about 3.8 per nm^2. Therefore, about $(1 - 1.8\ nm^{-2})/[(3.8\ nm^{-2}) \times 100\%] = 53\%$ of the inner surfaces of SBA-15/64 can be covered with aluminum. This value is quite reasonable because the Si/Al atomic ratio for this material is about 4 and aluminum is concentrated at the surface.

^1H MAS NMR spectra provide information on the accessibility of surface hydroxyl groups for guest molecules at room temperature, the presence of adsorbed water, and proton-exchange processes on silica surfaces. The position of the dominating resonance at 1.7 ppm, corresponding to isolated silanol groups,[29] directly indicates that both SBA-15/0 and SBA-15/64 silicas do not contain mobile adsorbed water after evacuation at 420 K. The presence of mobile water molecules promotes proton exchange between different species and results in a low-field shift of the resonance due to hydrogen bonding.[33−35] The disappearance of the resonance at 1.7 ppm in the presence of pyridine demonstrates that these isolated silanol groups are accessible to guest molecules. They form hydrogen bonds with pyridine that results in a low-field shift of the corresponding signal to 5−10 ppm. The increased line width of the low-field

resonance could arise from a local inhomogeneity in the pyridine distribution.

The broad signal at 3 ppm can be assigned to weakly interacting hydroxyl groups. At least some of these groups are not accessible to pyridine because the signal is observed in the presence of pyridine. The number of these hidden hydroxyl groups increases upon alumination. The interacting silanol groups are absent in MCM-41 materials free from structural defects.[24] Thus, we may presume for SBA-15/0 that the interacting silanol groups are disposed of on the surfaces of micropores whereas the surfaces of mesopores exclusively contain the isolated silanol groups. Although the signal at 3 ppm is too broad for its integral intensity to be measured accurately, it is apparently affected by pyridine to some extent. This can be explained as follows. A small number of pyridine molecules penetrates the micropores. At room temperature, these molecules diffuse rapidly along the surface, switching, breaking, and again forming hydrogen bonds with silanol groups. This results in a low-field shift of the ^{1}H resonance of the latter. At low temperature, pyridine molecules are immobilized and just a few molecules at the entrance of a micropore can block the rest of the pore volume. As a result, the effective surface area accessible to pyridine is reduced.

Surprisingly, the samples prepared by the loading of pyridine as a drop under an argon/nitrogen atmosphere do not provide any evidence that the alumination process results in the appearance of new Brønsted or Lewis acid groups on the silica surface. The resonance at 251 ppm observed for SBA-15/8-b and SBA-15/64-b can be tentatively attributed to an effect of the modification on the proton-donating ability of the surface silanol groups rather than to the appearance of hydroxyl groups interacting with aluminum atoms. Indeed, the ^{1}H NMR spectrum of SBA-15/64 shows the resonance characteristic of isolated pure silanol groups[29] (Figure 5d) and does not differ significantly from the spectra of nonaluminated SBA-15/0 (Figure 5a) whereas the acidic Al(OH)Si groups were found in zeolites to resonate at 4 ppm and below.[36] It is noteworthy that the interaction of pyridine with Brønsted acid sites should result in the formation of a strong hydrogen bond, where the mobile proton resonates at ca. 16 ppm.[37] However, the spectra obtained for pyridine adsorbed onto SBA-15/64 do not exhibit any signal outside the region shown up to 30 ppm.

At room temperature, pyridine molecules adsorbed onto mesoporous silica are in dynamic exchange between different phases and adsorption sites. This exchange is rapid on the NMR timescale and results in an observation of time-averaged signals from all presented species. When pyridine is loaded in excess, the position of the resonance is not very informative (Figure 2k,m). In contrast, the high-field shift of the ^{15}N NMR signals in SBA-15/8-a and SBA-15/64-a at 300 K as compared to that of the position at 130 K provides useful information. At room temperature, pyridine loaded onto SBA-15/0 can be in a rapid dynamic exchange either exclusively between different hydrogen-bonded sites or between the hydrogen-bonded state and the bulk phase. In the hydrogen-bonded state, pyridine resonates at 258 ppm, and in the bulk phase, at 276 ppm. The value of the experimentally observed ^{15}N chemical shift $\delta(^{15}N)_{av}$ depends on molar fractions x_{OH} and x_{free} of pyridine in the two states: $\delta(^{15}N)_{av} = (x_{OH})(258\ ppm) + (x_{free})(276\ ppm)$. The experimental value of $\delta(^{15}N)_{av}$ at 300 K is 258 ppm, that is, $x_{OH} = 1$ and $x_{free} = 0$. We conclude that when a submonolayer of pyridine is loaded onto mesoporous silicas, pyridine does not leave the surface at room temperature. For aluminated SBA-15/8 and SBA-15/64, it is reasonable to suggest that pyridine does not leave the surface even at higher temperatures, as also evidenced by FTIR measurements. Then, the simplest assumption is that pyridine can exchange between two different hydrogen-bonded states with signals at 258 and 251 ppm. That is, $\delta(^{15}N)_{av} = (x^{a}_{OH})(258\ ppm) + (x^{b}_{OH})(251\ ppm)$. For SBA-15/8-a and SBA-15/64-a samples, $\delta(^{15}N)_{av} = 251$ ppm at 300 K, although x^{a}_{OH}/x^{b}_{OH} is 1.86 and 1.25, respectively (Table 2). One can hardly imagine why pyridine molecules remain at room temperature exclusively in the minor hydrogen-bonded state characterized by the signal at 251 ppm. Most probably, the coincidence is accidental and there are some other states in which pyridine resonates below 251 ppm. However, something prevents the localization of pyridine at these sites at both room and low temperatures. Indeed, the ^{15}N spectrum of SBA-15/64-b that was kept for 60 days in a tightly closed NMR rotor reveals that new states, in which pyridine resonates at 233, 200, and 167 ppm, are formed at the expense of pyridine hydrogen bonded to silanol groups. Similar chemical shifts have been reported in the past for pyridine adsorbed on Lewis (226 and 198,[26] and 226 ppm[28]) and Brønsted (166[26] and 159 ppm[28]) acid sites of aluminated silica. Therefore, the following question arises: Why does it take so much time for pyridine to reach these acid sites although the resulting states should be more energetically favorable as compared to physisorbed pyridine? We attribute this effect to the features of the preparation procedures of these samples. We note that silica had been first dried in vacuo at 420 K and then placed in a glovebag under an argon/nitrogen atmosphere. It is known that nitrogen molecules interact relatively strong with Lewis acid sites and do not desorb from such sites at room temperature.[38] Thus, the Lewis sites turn out to be blocked by adsorbed nitrogen molecules before the addition of pyridine, and it takes a while before pyridine replaces nitrogen at the Lewis acid sites. The Brønsted acid sites are conventionally attributed to silanol groups interacting with Lewis acid sites. Nitrogen does not interact with Brønsted acids but presumably can inhibit this interaction that results in a drastic reduction in the proton-donating ability of the silanol groups.

In conclusion, the interpretation of the reported experimental results suggests that (i) the inner surfaces of the mesopores of SBA-15/0 contain cavities that are easily accessible to nitrogen but hardly accessible to pyridine; (ii) alumination results in a gradual filling of the cavities of rough mesopore walls that finally leads to aluminum islands on the inner surfaces of mesopores; (iii) in SBA-15 with the Si/Al atomic ratio equal to 4.1, up to half of the inner surface area of the mesopores is covered with aluminum; (iv) nitrogen strongly interacts with Lewis acid sites and inhibits the accessibility of these sites to other electron donors; and (v) at room temperature, it takes days before stronger bases such as pyridine can replace chemically adsorbed nitrogen.

4.2. Interaction of the SBA-15 Surface with Pyridine Loaded by Vacuum Transfer. The loading of pyridine onto aluminated silica by vacuum transfer provides both a homogeneous distribution of the guest molecules on the surface and their unrestricted interaction with Brønsted and Lewis acid sites. The integral intensities of ^{15}N NMR signals at 258, 200, and 167 ppm of sample SBA-15/8-c (Figure 4a) indicate that the total density of chemically active sites on the surface of SBA-15/8 silica is about 3.7 per nm^2 and among them are 2.7 weakly acidic silanol groups and 0.2 Lewis and 0.8 Brønsted acid sites, respectively

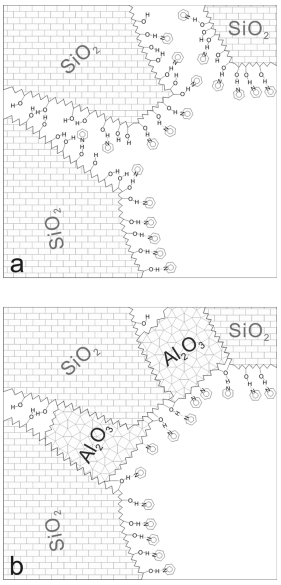

Figure 6. (a) Schematic representation of the structure of the purely siliceous SBA-15/0 material and the effect of alumination. Silanol groups of mesopores of SBA-15/0 are accessible to pyridine molecules at any temperature, and the entrances into the cavities of rough mesopore walls can be blocked by a few pyridine molecules at low temperature. (b) Al species most effectively react with the silica surface in the strongly confined geometry of the cavities instead of forming a homogeneous film at the surface.

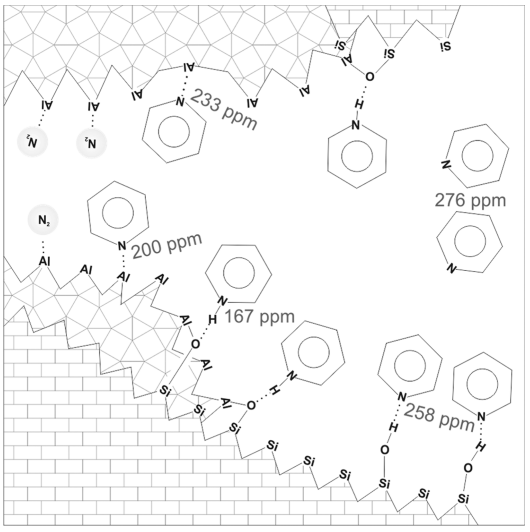

Figure 7. Schematic representation of the species formed by pyridine with Brønsted and Lewis acid sites on the surface of aluminated SBA-15. The species can be discriminated using the ^{15}N chemical shift of pyridine: bulk pyridine (276 ppm), pyridine hydrogen bonded to isolated silanol groups (258 ppm), pyridine bound to penta- (233 ppm) and tetracoordinated (200 ppm) aluminum, and pyridine protonated by silanol group interacting with aluminum (167 ppm). The chemical shifts are referenced to the solid $^{15}NH_4Cl$ scale.

(Table 2). Upon an increase in the Al content, the number of weakly acidic silanol groups decreases whereas the number of Lewis acid sites strongly increases (sample SBA-15/64-c). Moreover, there are now two different types of Lewis acid sites observed. The relative concentrations of these sites are roughly the same, as can be concluded from the integral intensities of the ^{15}N NMR signals at 233 and 200 ppm (Figure 4b). Taking into account the results of ^{27}Al NMR experiments previously reported for SBA-15/8 and SBA-15/64 samples,[21] we attribute the resonances at 233 and 200 ppm to pyridine molecules located at penta- and tetracoordinated aluminum, respectively.

A comparison of the numerical data obtained for SBA-15/64-c and SBA-15/64-d samples suggests that the number of Lewis and Brønsted acid sites on the surface of aluminated silica depends on the temperature at which the material has been annealed. The samples have been evacuated at 700 and 420 K, respectively, and pyridine has been loaded in both cases at the temperature of liquid nitrogen. The reduction of the annealing temperature results in a 4-fold decrease in the concentrations of the Lewis acid sites of both types and a 3-fold increase in the concentration of the Brønsted acid sites. The latter seems to happen at the expense of the weakly acidic silanol groups (Table 2). We attribute these findings to morphological changes in the surface of aluminated silica upon annealing at 700 K. We expect that these changes result in a reduction in the number of silanol groups interacting with aluminum. Besides, octahedral aluminum can be partially converted to tetra- or pentacoordinated aluminum. SBA-15/64 silica used for both samples was calcined at 810 K.[21] Thus, these changes should be reversible, although the relaxation rate can be slow in the absence of water. The total numbers of the two types of Brønsted acid groups and the two types of Lewis acid groups in SBA-15/64-c sample are roughly equal. This finding supports our estimations that in the material with a Si/Al atomic ratio of 4.1 up to half of the inner surface area of the mesopores is covered with aluminum.

In conclusion, the interpretation of the reported experimental results suggests that (i) the Lewis and Brønsted acid sites of aluminated SBA-15 are accessible to pyridine when the surface does not contain other strongly bound electron donors; (ii) the numbers of Lewis and Brønsted acid sites depend on the temperature at which the material has been annealed; (iii) there are two types of the Lewis acid sites that are attributed to penta- and tetracoordinated aluminum.

4.3. Surface Roughness. Is the absence of a measurable residual anisotropy of the ^{15}N NMR chemical shift of the adsorbed pyridine indicative of the considerable roughness of the surface even after alumination, in contrast to the statement in ref 21? This question cannot be answered straightforwardly because of the features of the host−guest interaction in the concerned case. The critical requirement for the use of ^{15}N NMR of pyridine to estimate the surface roughness is the hindrance of pyridine rotation around the molecular C_2 axis.[24] Hydrogen bonding to the surface silanol groups provides such a hindrance because pyridine has to be oriented along the O−H bond; that is, the angle between the Si−O bond and the molecular C_2 axis is about 140°.[24] In contrast, when pyridine is protonated by the silanol group, this angle is close to 180° and the surface does not affect the rotation. In this case, the spectral line in the static ^{15}N NMR spectrum is isotropic even when the protonated pyridine is immobilized at a certain surface group.[18] On the partially aluminated surface, both the diffusion along the rough surface and the rotation around the molecular C_2 axis during the location at Lewis acid sites can result in the averaging of the anisotropy of the ^{15}N NMR chemical shift tensor of pyridine. The available NMR data are insufficient to decide which of the two factors plays the major role.

dx.doi.org/10.1021/la2017566 |*Langmuir* 2011, 27, 12115–12123

5. CONCLUSIONS

Figure 6 schematically depicts the structure of purely siliceous SBA-15/0 material and the effect of alumination on the structural features. These cartoons exhibit features found experimentally for purely siliceous SBA-15/0 and aluminated SBA-15/8 and SBA-15/64 materials. Our interpretations of the ^{1}H and variable-temperature ^{15}N NMR spectra of these materials loaded with pyridine can be summarized as follows. The corona around the mesopores of the SBA-15/0 material has micropores (surface roughness or cavities) that are easily accessible to nitrogen but not to pyridine. Although at room temperature most of the silanol groups of these micropores are still accessible to pyridine, at low temperature a few pyridine molecules can block the entrance into a cavity. The proton-donating ability of the silanol groups of the mesopores of SBA-15/0 is comparable to the proton-donating ability of an acid, exhibiting an apparent pK_a value of about 5.0. The N···H distance in the pyridine−silanol pairs is about 1.7 Å. Aluminum chlorhydrol most effectively reacts with silica surface in the confinement of the cavities instead of forming a homogeneous film at the surface. Thus, the alumination results in a gradual smoothing of the mesopore surface and finally leads to aluminum islands on the inner surfaces of the mesopores. This conclusion is supported by the ^{15}N NMR data of this work and the interpretation of adsorption data in ref 21. In the material with a Si/Al atomic ratio of 4.1, up to a half of the inner surface area of the mesopores is covered with aluminum.

The most intriguing result of the current study is that gaseous nitrogen can occupy Lewis acid sites and hinder the interaction of aluminum with any other electron donor. As a result, the aluminated surface saturated with nitrogen does not exhibit any Brønsted or Lewis acidity. At room temperature, it takes days before pyridine replaces nitrogen at the Lewis acid sites. Future experimental studies will be necessary in order to understand the reason that this exchange occurs so unbelievably slowly. Evacuation at 420 K is sufficient to remove the adsorbed nitrogen. Such a surface exhibits up to two types of Brønsted and Lewis acid groups each (Figure 7). The presence of these sites is in agreement with the available FTIR data[39−45] and some other NMR studies.[26,28,46,47] Isolated silanol groups are responsible for the physisorption of pyridine on silica surfaces. The proton-donating ability of silanol groups interacting with aluminum is sufficient to protonate pyridine. At low aluminum content, the surface contains Lewis acid sites with a high acidity. These sites are attributed to tetracoordinated aluminum. The ^{15}N NMR signal of pyridine interacting with the tetracoordinated aluminum is located at 200 ppm. An increase in aluminum content results in the appearance of Lewis acid sites of a lower acidity attributed to pentacoordinated aluminum. Pyridine adsorbed on these sites resonates at 233 ppm.

AUTHOR INFORMATION

Corresponding Author

*(J.Č.) E-mail: jiri.cejka@jh-inst.cas.cz. Tel: +42 266053795. Fax: +42 286582307. (I.G.S.) E-mail: shender@chemie.fu-berlin.de. Tel: +49 (0) 30 83853615. Fax: +49 (0) 30 83855310.

ACKNOWLEDGMENT

This work was supported by the Deutsche Forschungsgemeinschaft, the German-Russian Interdisciplinary Science Center (G-RISC), the Russian Foundation of Basic Research (09-03-91336), and contract 02.740.11.0214. A.Z. and J.Č. thank the Academy of Sciences of the Czech Republic (KAN 100400701) and the Grant Agency of the Czech Republic (203/08/0604) for their support.

REFERENCES

(1) Morell, J.; Chatterjee, S.; Klar, P. J.; Mauder, D.; Shenderovich, I.; Hoffmann, F.; Froba, M. *Chem.—Eur. J.* **2008**, *14*, 5935–5940.
(2) Taguchi, A.; Schüth, F. *Microporous Mesoporous Mater.* **2004**, *77*, 1–45.
(3) Øye, G.; Sjöblom, J.; Stöcker, M. *Adv. Synth. Catal.* **2001**, *89−90*, 439–466.
(4) Parida, S. K.; Dash, S.; Patel, S.; Mishra, B. K. *Adv. Colloid Interface Sci.* **2006**, *121*, 77–110.
(5) Corma, A.; Garcia, H. *Adv. Synth. Catal.* **2006**, *348*, 1391–1412.
(6) Martín-Aranda, R. M.; Čejka, J. *Top. Catal.* **2010**, *53*, 141–153.
(7) Akcakayiran, D.; Mauder, D.; Hess, C.; Sievers, T. K.; Kurth, D. G.; Shenderovich, I. G.; Limbach, H.-H.; Findenegg, G. H. *J. Phys. Chem. B* **2008**, *112*, 14637–14647.
(8) Mauder, D.; Akcakayiran, D.; Lesnichin, S. B.; Findenegg, G. H.; Shenderovich, I. G. *J. Phys. Chem. C* **2009**, *113*, 19185–19192.
(9) Brunel, D.; Blanc, A. C.; Galarneau, A.; Fajula, F. *Catal. Today* **2002**, *73*, 139–152.
(10) Trombetta, M.; Busca, G.; Lenarda, M.; Storaro, L.; Pavan, M. *Appl. Catal., A* **1999**, *182*, 225–235.
(11) Hunger, M.; Schenk, U.; Breuninger, M.; Gläser, R.; Weitkamp, J. *Microporous Mesoporous Mater.* **1999**, *27*, 261–271.
(12) Dědeček, J.; Žilková, N.; Čejka, J. *Microporous Mesoporous Mater.* **2001**, *44−45*, 259–266.
(13) Xu, M.; Wang, W.; Seiler, M.; Buchholz, A.; Hunger, M. *J. Phys. Chem. B* **2002**, *106*, 3202–3208.
(14) Luo, Q.; Deng, F.; Yuan, Z.; Yang, J.; Zhang, M.; Yue, Y.; Ye, C. *J. Phys. Chem. B* **2003**, *107*, 2435–2442.
(15) Hu, W.; Luo, Q.; Su, Y.; Chen, L.; Yue, Y.; Ye, C.; Deng, F. *Microporous Mesoporous Mater.* **2006**, *92*, 22–30.
(16) Wang, Y.; Lang, N.; Tuel, A. *Microporous Mesoporous Mater.* **2006**, *93*, 46–54.
(17) Góra-Marek, K.; Derewiński, M.; Sarv, P.; Datka, J. *Catal. Today* **2005**, *101*, 131–138.
(18) Ip, B. C. K.; Andreeva, D. V.; Buntkowsky, G.; Akcakayiran, D.; Findenegg, G. H.; Shenderovich, I. G. *Microporous Mesoporous Mater.* **2010**, *134*, 22–28.
(19) Mokaya, R. *Chem. Commun.* **2000**, 1891–1892.
(20) Zukal, A.; Mayerová, J.; Čejka, J. *Phys. Chem. Chem. Phys.* **2010**, *12*, 5240–5247.
(21) Zukal, A.; Šiklová, H.; Čejka, J. *Langmuir* **2008**, *24*, 9837–9842.
(22) Shenderovich, I. G.; Mauder, D.; Akcakayiran, D.; Buntkowsky, G.; Limbach, H.-H.; Findenegg, G. H. *J. Phys. Chem. B* **2007**, *111*, 12088–12096.
(23) Lorente, P.; Shenderovich, I. G.; Golubev, N. S.; Denisov, G. S.; Buntkowsky, G.; Limbach, H.-H. *Magn. Reson. Chem.* **2001**, *39*, S18–S29.
(24) Shenderovich, I. G.; Buntkowsky, G.; Schreiber, A.; Gedat, E.; Sharif, S.; Albrecht, J.; Golubev, N. S.; Findenegg, G. H.; Limbach, H.-H. *J. Phys. Chem. B* **2003**, *107*, 11924–11939.
(25) Lesnichin, S. B.; Kamdem, N.; Mauder, D.; Denisov, G. S.; Shenderovich, I. G. *Russ. J. Gen. Chem.* **2010**, *80*, 2027–2031.
(26) Ripmeester, J. A. *J. Am. Chem. Soc.* **1983**, *105*, 2925–2927.
(27) Maciel, G. E.; Haw, J. F.; Chuang, I.-S.; Hawkins, B. L.; Early, T. A.; McKay, D. R.; Petrakis, L. *J. Am. Chem. Soc.* **1983**, *105*, 5529–5535.
(28) Haw, J. F.; Chuang, I.-S.; Hawkins, B. L.; Maciel, G. E. *J. Am. Chem. Soc.* **1983**, *105*, 7206–7207.
(29) Anwander, R.; Nagl, I.; Widenmeyer, M.; Engelhardt, G.; Groeger, O.; Palm, C.; Röser, Th. *J. Phys. Chem. B* **2000**, *104*, 3532–3544.
(30) Emeis, C. A. *J. Catal.* **1993**, *141*, 347–354.

(31) Andreeva, D. V.; Ip, B.; Gurinov, A.; Tolstoy, P. M.; Shenderovich, I. G.; Limbach, H.-H. *J. Phys. Chem. A* **2006**, *110*, 10872–10879.
(32) Sharif, S.; Shenderovich, I. G.; Gonzalez, L.; Denisov, G. S.; Silverman, D. N.; Limbach, H.-H. *J. Phys. Chem. A* **2007**, *111*, 6084–6093.
(33) Gruenberg, B.; Emmler, Th.; Gedat, E.; Shenderovich, I. G.; Findenegg, G. H.; Limbach, H.-H.; Buntkowsky, G. *Chem.—Eur. J.* **2004**, *10*, 5689–5696.
(34) Limbach, H. H.; Tolstoy, P. M.; Perez-Hernandez, N.; Guo, J.; Shenderovich, I. G.; Denisov, G. S. *Isr. J. Chem.* **2009**, *49*, 199–216.
(35) Pizzanelli, S.; Kababya, S.; Frydman, V.; Landau, M.; Vega, S. *J. Phys. Chem. B* **2005**, *109*, 8029–8039.
(36) Hunger, M.; Freude, D.; Pfeifer, H. *J. Chem. Soc., Faraday Trans.* **1991**, *87*, 657–662.
(37) Hunger, M. *Solid State Nucl. Magn. Reson.* **1996**, *6*, 1–29.
(38) Wakabayashi, F.; Kondo, J.; Wada, A.; Domen, K.; Hirose, C. *J. Phys. Chem.* **1993**, *97*, 10761–10768.
(39) Gallo, J. M. R.; Bisio, C.; Gatti, G.; Marchese, L.; Pastore, H. O. *Langmuir* **2010**, *26*, 5791–5800.
(40) Handjani, S.; Dzwigaj, S.; Blanchard, J.; Marceau, E.; Kraft, J.-M.; Che, M. *Top. Catal.* **2009**, *52*, 334–343.
(41) Dragoi, B.; Dumitriu, E.; Guimon, C.; Auroux, A. *Microporous Mesoporous Mater.* **2009**, *121*, 7–17.
(42) Gomez-Cazalilla, M.; Merida-Robles, J. M.; Gurbani, A.; Rodriguez-Castellon, E.; Jimenez-Lopez, A. *J. Solid State Chem.* **2007**, *180*, 1130–1140.
(43) Oumi, Y.; Takagi, H.; Sumiya, S.; Mizuno, R.; Uozumi, T.; Sano, T. *Microporous Mesoporous Mater.* **2001**, *44*−*45*, 267–274.
(44) Sumiya, S.; Oumi, Y.; Uozumi, T.; Sano, T. *J. Mater. Chem.* **2001**, *11*, 1111–1115.
(45) Gedeon, A.; Lassoued, A.; Bonardet, J. L.; Fraissard, J. *Microporous Mesoporous Mater.* **2001**, *44*−*45*, 801–806.
(46) Marthala, V. R. R.; Rabl, S.; Huang, J.; Rezai, S. A. S.; Thomas, B.; Hunger, M. *J. Catal.* **2008**, *257*, 134–141.
(47) Marthala, V. R. R.; Frey, J.; Hunger, M. *Catal. Lett.* **2010**, *135*, 91–97.